Upper Bound to the Orbital Angular Momentum Carried by an Ultrashort Pulse

Miguel A. Porras*
Grupo de Sistemas Complejos, ETSIME, Universidad Politécnica de Madrid, Rios Rosas 21, 28003 Madrid, Spain

(Received 31 December 2018; published 29 March 2019)

Photons in a ring-shaped vortex light beam can have an arbitrarily high orbital angular momentum (OAM) $l\hbar$, in addition to the spin angular momentum $\pm\hbar$. For a pulsed vortex beam, there is, however, an upper bound to the integer units l of OAM, or topological charge of the vortex, and a lower bound to the pulse duration to carry OAM. These limits have implications in experiments with ultrashort vortices, e.g., in the generation of twisted attosecond bursts in the extreme ultraviolet, in the temporal resolution in ultrafast spectroscopy, or in the performance of OAM-based optical communications or cryptographic systems, as well as in other areas of physics as acoustics or electron waves.

DOI: 10.1103/PhysRevLett.122.123904

An optical vortex beam is a light beam with a phase variation $e^{-il\phi}$ in the azimuthal direction ϕ perpendicular to the propagation direction of the beam, say, z. At the beam center, $r = 0$, the phase is undetermined, and the optical field strength vanishes, which endows the beam with a ring structure. The integer number l, called a topological charge, can take arbitrarily high positive or negative values and determines the orbital angular momentum (OAM) $l\hbar$ per photon of the beam [1,2]. Archetypical vortex beams are Laguerre-Gauss (LG) beams, easily produced using fork-type gratings or spiral phase plates [2]. Recognizing the existence of these new and unlimited degrees of freedom of the photons in a beam as familiar as a LG beam [1] was a substantial advance in optics with ramifications in other fields such as astrophysics [3] or medicine [4], with applications such as optical tweezers [5], laser ablation [6], or classical and quantum information processing [7,8]. The unboundedness of l seems to be corroborated by the feasibility of generating beams with up to $10^4\hbar$ OAM per photon [9].

With ultrashort pulses, these applications acquire, in addition, ultrafast resolution. The generation of shorter and shorter ring-shaped pulses carrying vortices has had to overcome practical difficulties such as the spatial, group velocity, and topological charge dispersion introduced by gratings and spiral phase plates [10–12]. Nonetheless, the few-cycle regime has already been achieved [13,14], and in strong-field physics these ring-shaped pulses are used to excite high harmonics and extremely short attosecond pulses with vortices of high topological charge [15–17].

In this Letter, we show that there is a fundamental restriction to the topological charge of the vortex, and hence to the OAM, carried by a pulse. As a reference, the topological charge of a single-cycle pulse (according to the standard definition [18]) is $|l| = 27$ as much. This restriction implies that there exist minimal wave packets able to carry an l-charged vortex. In Ref. [19], a limitation to the OAM in a single-cycle (subcycle according to Ref. [18]) X wave with an exponentially decaying spectrum is described. Intuitively, the idea of unlimited OAM, involving an arbitrary number of intertwined helical phase fronts in the case of monochromatic LG beams [2], is hardly reconciled with arbitrarily short pulses, for which the concept of phase fades away. Here, a proof of a precise limit for general pulse shapes in the actual beam geometries in experiments is provided.

Suppose we have overcome all the technical difficulties [10–12] and synthesized the ring pulsed beam (RPB)

$$E(r,\phi,z,t') = \frac{1}{\pi}\int_0^\infty \hat{E}_\omega(r,\phi,z)e^{-i\omega t'}d\omega, \tag{1}$$

as the superposition of LG beams

$$\hat{E}_\omega(r,\phi,z) = \hat{a}_\omega \frac{e^{-i(|l|+1)\psi_\omega(z)}e^{-il\phi}}{\sqrt{1+(\frac{z}{z_{R,\omega}})^2}}\left(\frac{\sqrt{2}r}{s_\omega(z)}\right)^{|l|} e^{i\omega r^2/[2cq_\omega(z)]}, \tag{2}$$

all them of the same topological charge l, and zero radial order, but different frequencies ω and weights $\hat{a}_\omega$. In the above equations, and in the introduction, (r,ϕ,z) are cylindrical coordinates, $t' = t - z/c$ is the local time, c is the speed of light in a vacuum, $q_\omega(z) = z - iz_{R,\omega}$ is the complex beam parameter, $\psi_\omega(z) = \tan^{-1}(z/z_{R,\omega})$, $s_\omega(z) = s_\omega\sqrt{1+(z/z_{R,\omega})^2}$, $s_\omega = \sqrt{2z_{R,\omega}c/\omega}$ is the waist width of the fundamental Gaussian beam ($l = 0$), and $z_{R,\omega}$ is the Rayleigh distance. Additionally, the complex beam parameter is usually written as

$$\frac{1}{q_\omega(z)} = \frac{1}{R_\omega(z)} + i\frac{2c}{\omega s_\omega^2(z)}, \tag{3}$$

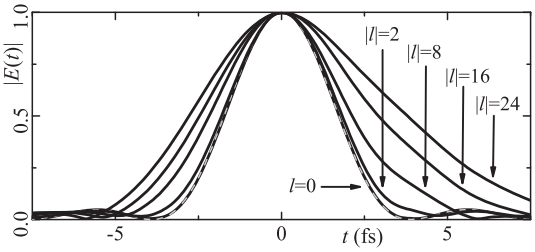

FIG. 1. Propagation of the pulsed LG disturbance $E(r,\phi,0,t) = P(t)(\sqrt{2}r/s)^{|l|}\exp(-r^2/s^2)\exp(-il\phi)$. Dashed gray curve: Envelope of the single-cycle pulse $P(t) = \mathrm{sinc}^2(t/T)\exp(-i\omega_0 t)$, $\omega_0 = 2.417$ fs^{-1}, and $T = 3.9$ fs. Black curves: For the indicated values of $|l|$, a pulse envelope at the bright ring at one Rayleigh distance. Peak values are set to unity and shifted to $t = 0$ for better comparison.

where $1/R_\omega(z) = z/(z^2 + z_{R,\omega}^2)$ is the curvature of the wave fronts. Being limited to positive frequencies, the optical field E in Eq. (1) is the analytical complex representation of the real optical field $\mathrm{Re}\{E\}$ [20]. Since Eq. (1) vanishes at $r = 0$ and $r \to \infty$, it will feature a bright ring about a certain radius. It is natural to identify, from both a theoretical and an applicative point of view, the pulse shape of the RPB with that at the bright ring, or at the brightest if there are several. As said, we analyze if this pulse shape and the topological charge l can be taken arbitrarily or there is some kind of restriction.

A prerequisite to talk about the pulse shape of a vortex-carrying pulse is that it remains unchanged during propagation (except for a global complex amplitude, as usually understood). Figure 1 illustrates the situation with the usual model with a factorized field in space and time at the focus or waist $z = 0$, in which the Gaussian waist width $s_\omega \equiv s$ is independent of the frequency [15]. While for a few-cycle pulsed Gaussian beam ($l = 0$) the pulse shape on its maximum (at $r = 0$) is substantially unaltered [21,22], the same few-cycle pulse on the bright ring of a RPB widens and distorts, particularly for high $|l|$, as seen in Fig. 1. The origin of this distortion is a dispersion, particularly enhanced for high $|l|$ and for short pulses, induced by Gouy's phase when $z_{R,\omega}$ depends on the frequency, as it is in the factorized model. Similar dispersion affects at sufficiently high $|l|$ the pulse shape in any other model in which $z_{R,\omega}$ depends on the frequency. Thus, the so-called isodiffracting model [23–26] in which $z_{R,\omega} \equiv z_R$ is independent of the frequency becomes particularly relevant as the only type of RPB for which an ultrashort pulse can maintain its shape during propagation irrespective of the value of $|l|$. With ω-independent z_R, $\psi_\omega(z) \equiv \psi(z)$, $q_\omega(z) \equiv q(z)$, and $R_\omega(z) \equiv R(z)$ are also ω independent, and the Gaussian width $s_\omega(z)$ is inversely proportional to the square root ω.

For our analysis, we introduce the diffraction and azimuthal factor $D(z,\phi) = e^{-il\phi}e^{-(|l|+1)\psi(z)}/\sqrt{1+(z/z_R)^2}$ and the scaled radius $\rho = r/\sqrt{2z_R c[1+(z/z_R)^2]}$ at each distance z. The constant ρ represents a hyperboloid of revolution about the z axis, also called a caustic surface, along which the ring pulse spreads. Using Eq. (3) and the expressions of $s_\omega(z)$ and s_ω above, the integral in Eq. (1) with Eq. (2) is conveniently written as

$$E = D(\sqrt{2}\rho)^{|l|}\frac{1}{\pi}\int_0^\infty \hat{a}_\omega \omega^{|l|/2} e^{-\rho^2\omega} e^{-i\omega t''} d\omega, \qquad (4)$$

where $t'' \equiv t' - r^2/2cR(z)$ and where it is seen that the pulse shape depends on the particular caustic surface ρ but does not change on propagation, being only attenuated by the diffraction factor in D. If at $z = 0$ the pulse peaks at the time $t' = 0$, it does at $z \neq 0$ at the time determined by $t'' = t' - r^2/2cR(z) = 0$, which defines a spherical pulse front of radius $R(z)$ at each distance z.

We first find the expression of a RPB with a certain pulse shape $P(t) = (1/\pi)\int_0^\infty \hat{P}_\omega e^{-i\omega t} d\omega$ and frequency spectrum $\hat{P}_\omega$ at a particular caustic surface ρ_p. Equating Eq. (4) particularized at ρ_p to $DP(t)$, we get $\hat{a}_\omega = e^{\rho_p^2\omega}\omega^{-|l|/2}(\sqrt{2}\rho_p)^{-|l|}\hat{P}_\omega$, and Eq. (4) becomes

$$\begin{aligned} E &= D\left(\frac{\rho}{\rho_p}\right)^{|l|}\frac{1}{\pi}\int_0^\infty \hat{P}_\omega e^{-(\rho^2-\rho_p^2)\omega} e^{-i\omega t''} d\omega \\ &= D\left(\frac{\rho}{\rho_p}\right)^{|l|} P[t'' - i(\rho^2 - \rho_p^2)]. \end{aligned} \qquad (5)$$

Its spectrum $\hat{E}_\omega = D(\rho/\rho_p)^{|l|}\hat{P}_\omega e^{-(\rho^2-\rho_p^2)\omega}$ at $\rho > \rho_p$ ($\rho < \rho_p$) is a redshifted (blueshifted) version of $\hat{P}_\omega$.

Next, we identify the bright caustic surface as that where the pulse energy is maximum. The energy per unit transverse area, or fluence, is given by $\mathcal{E}(r,z) = \int_{-\infty}^{\infty}(\mathrm{Re}E)^2 dt = (1/2)\int_{-\infty}^{\infty}|E|^2 dt = (1/\pi)\int_0^\infty |\hat{E}_\omega|^2 d\omega$ and for the RPB in Eq. (5) by

$$\mathcal{E} = |D|^2\left(\frac{\rho}{\rho_p}\right)^{2|l|}\frac{1}{\pi}\int_0^\infty |\hat{P}_\omega|^2 e^{-2(\rho^2-\rho_p^2)\omega} d\omega. \qquad (6)$$

Differentiating with respect to ρ, we obtain, after some algebra, $d\mathcal{E}/d\rho = \mathcal{E}[2|l| - 4\rho^2\bar{\omega}(\rho)]/\rho$, where

$$\bar{\omega}(\rho) = \frac{\int_0^\infty |\hat{P}_\omega|^2 e^{-2(\rho^2-\rho_p^2)\omega}\omega d\omega}{\int_0^\infty |\hat{P}_\omega|^2 e^{-2(\rho^2-\rho_p^2)\omega} d\omega} \qquad (7)$$

is the mean frequency of the pulse at the caustic ρ. Thus, a caustic surface ρ_s of maximum or minimum energy density satisfies $\rho_s^2 = |l|/2\bar{\omega}(\rho_s)$. The second derivative of the energy profile can be similarly evaluated and, at the maxima or minima $\rho_s^2 = |l|/2\bar{\omega}(\rho_s)$, is given by $d^2\mathcal{E}/d\rho^2|_{\rho_s} = -8\mathcal{E}(\rho_s)\bar{\omega}(\rho_s)\{1 - |l|[\sigma^2(\rho_s)/\bar{\omega}^2(\rho_s)]\}$, where

$$\sigma^2(\rho) = \frac{\int_0^\infty |\hat{P}_\omega|^2 e^{-2(\rho^2-\rho_p^2)\omega}[\omega - \bar{\omega}(\rho)]^2 d\omega}{\int_0^\infty |\hat{P}_\omega|^2 e^{-2(\rho^2-\rho_p^2)\omega} d\omega} \tag{8}$$

is the variance of the pulse spectrum at each caustic ρ. Thus, the caustic ρ_s has a maximum of energy if $|l| < \bar{\omega}^2(\rho_s)/\sigma^2(\rho_s)$ and a minimum if $|l| > \bar{\omega}^2(\rho_s)/\sigma^2(\rho_s)$.

Then, for $P(t)$ to be the pulse shape at a caustic of maximum or minimum energy, it must be located at $\rho_p^2 = |l|/2\bar{\omega}$, where $\bar{\omega} \equiv \bar{\omega}(\rho_p)$ is the mean frequency of $P(t)$. The caustic is of maximum pulse energy if

$$|l| < \bar{\omega}^2/\sigma^2, \tag{9}$$

where $\sigma^2 \equiv \sigma^2(\rho_p)$ is the variance of the pulse spectrum, and of minimum energy if $|l| > \bar{\omega}^2/\sigma^2$. In the latter case, for a continuous energy profile vanishing at $\rho = 0$ and at $\rho \to \infty$, there must exist at least two maxima ρ_s surrounding the minimum at ρ_p. In any of these maxima, e.g., the global maximum, the condition of maximum $|l| < \bar{\omega}^2(\rho_s)/\sigma^2(\rho_s)$ is satisfied by the pulse shape at that maximum. In conclusion, all RPBs verify restriction (9) between its topological charge and the pulse shape at its bright ring.

With the unscaled radius r, the bright caustic $\rho_p^2 = |l|/2\bar{\omega}$ reads $r_p = \sqrt{|l|/2}s_{\bar{\omega}}(z)$, where $s_{\bar{\omega}}(z) = s_{\bar{\omega}}\sqrt{1+(z/z_R)^2}$ and $s_{\bar{\omega}} = \sqrt{2z_R c/\bar{\omega}}$. Also, expression (5) with $\rho_p^2 = |l|/2\bar{\omega}$ can more explicitly be written, using Eq. (3) for the frequency $\bar{\omega}$, as

$$E(r,\phi,z,t') = \frac{e^{-i(|l|+1)\psi(z)}e^{-il\phi}}{\sqrt{1+(\frac{z}{z_R})^2}}\left(\sqrt{\frac{2}{|l|}}\frac{r}{s_{\bar{\omega}}(z)}\right)^{|l|} \times P\left(t' - \frac{r^2}{2cq(z)} + i\frac{|l|}{2\bar{\omega}}\right). \tag{10}$$

This equation describes a RPB of pulse shape $P(t)$ of maximum energy at $r_p = \sqrt{|l|/2}s_{\bar{\omega}}(z)$ if $P(t)$ is chosen to satisfy $\sigma^2/\bar{\omega}^2 < 1/|l|$. Otherwise, Eq. (10) is only an unpractical way to specify a RPB of a different pulse shape of maximum energy such that $\sigma^2/\bar{\omega}^2 < 1/|l|$ at another location. We stress that inequality (9) holds for arbitrarily short pulse forms, not only those having a physically meaningful carrier frequency $\bar{\omega}$ and envelope $A(t) = P(t)e^{i\bar{\omega}t}$, i.e., at least one carrier oscillation in the FWHM of $|P(t)|^2$ [18]. Restriction (9) involves only the spectral density $|\hat{P}_\omega|^2$ and not other characteristics such as the pulse duration. In particular, the topological charge is equally limited for a transform-limited pulse and for a temporally broadened pulse with inhomogeneous spectral phases. Also, the square root of the variance, σ, is usually too small to measure the pulse bandwidth, even the half bandwidth, but $\Delta\omega \equiv 2\sigma$ is the so-called Gaussian-equivalent half width ($1/e^2$ decay for Gaussian-like $|\hat{P}_\omega|^2$). In terms of $\Delta\omega$, inequality (9) reads $|l| < 4\bar{\omega}^2/\Delta\omega^2$.

Figure 2 is an example that helps to understand the precise meaning of this result. We try to synthesize RPBs of increasing topological charge but fixed pulse shape at their bright ring, the single-cycle pulse in Fig. 2(a). For this pulse, $|l|$ must be smaller than $\bar{\omega}^2/\sigma^2 = 22.5$. Figure 2(b) represents energy profiles for different values of $|l|$, with the vertical lines of the same color placed at $r/s_{\bar{\omega}}(z) = \sqrt{|l|/2}$. With low $|l|$, the energy has a single maximum at the expected radius $r/s_{\bar{\omega}}(z) = \sqrt{|l|/2}$ (red). A secondary

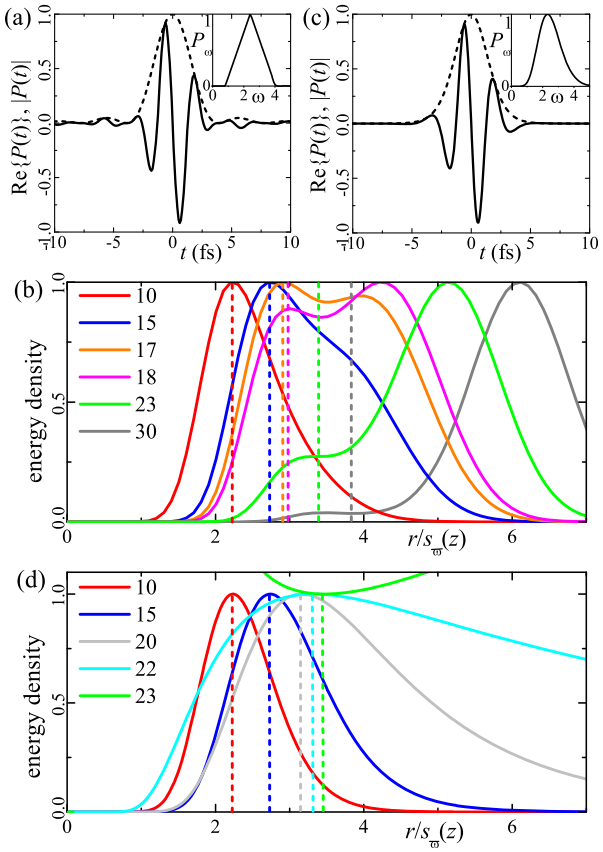

FIG. 2. (a) Real pulse and envelope of $P(t) = \mathrm{sinc}^2(t/T)\exp(-i\omega_0 t - i\pi/2)$ with $\omega_0 = 2.417$ fs^{-1} (780 nm wavelength) and $T = 3.9$ fs [single-cycle pulse with one carrier period $2\pi/\omega_0$ in its FWHM of intensity $|P(t)|^2$]. Its spectrum $\hat{P}_\omega = (T/2)\mathrm{tri}[2T(\omega-\omega_0)/\pi]$ (normalized to its peak value) is shown in the inset [$\mathrm{sinc}(x) \equiv \sin(\pi x)/\pi x$, and $\mathrm{tri}(x) \equiv 1 - x$ in $0 < x < 1$, $1 + x$ in $-1 < x < 0$, and 0 for $|x| > 1$]. For this pulse, $\bar{\omega} = \omega_0$ and $\sigma^2 = 0.26$ fs^{-2}, yielding $|l| < \bar{\omega}^2/\sigma^2 = 22.5$. (b) Energy profiles (normalized to the peak value in each case) of the RPBs in Eq. (10) with the indicated values of $|l|$. The vertical dashed lines are placed at $\sqrt{|l|/2}$. (c) Real part and modulus of $P(t)$ in Eq. (11) with $\bar{\omega} = 2.417$ fs^{-1}, $\alpha = 11.25$ (slightly subcycle pulse) and $\Phi = \pi/2$, and its spectrum in the inset. For this pulse, $\sigma^2 = 0.26$ fs^{-2}, and $|l| < \bar{\omega}^2/\sigma^2 = 22.5$, as in (a). (d) The same as in (b) but for the pulse in (c).

hump begins to emerge with $|l| \simeq 15$ (blue) and becomes a maximum with $|l| = 17$ (orange), and the absolute maximum with $|l| = 18$ (purple), while the original maximum remains at $r/s_{\bar{\omega}}(z) = \sqrt{|l|/2}$. With $|l| = 23$ (green), the maximum at $r/s_{\bar{\omega}}(z) = \sqrt{|l|/2}$ turns, as predicted, into a minimum, because a new, very weak maximum emerges on its left. This example confirms the validity of inequality (9) and illustrates that this inequality is not sharp in this example, but there is a lower upper bound $|l| < 18$ for this pulse.

This observation poses the question of whether there exist optimal OAM carrier pulses for which inequality (9) is sharp, i.e., $|l|$ can reach the integer part of $\bar{\omega}^2/\sigma^2$. We have found that this is the case of the pulses

$$P(t) = \left(\frac{-i\alpha}{\bar{\omega}t - i\alpha}\right)^{\alpha+1/2} e^{-i\Phi}, \tag{11}$$

with $\alpha > 1/2$ and Φ an arbitrary phase. Equation (11) is a convenient way to express the commonly used pulses with the power-exponential (PE) spectrum [19,24,25] $\hat{P}_\omega \propto (\omega/\bar{\omega})^{\alpha-1/2} e^{-\alpha\omega/\bar{\omega}} e^{-i\Phi}$, where the mean frequency appears explicitly. The pulse shape is fully determined by the parameter α and then scaled by $\bar{\omega}$. The (Gaussian-equivalent) half bandwidth $\Delta\omega = 2\sigma = \sqrt{2/\alpha}\,\bar{\omega}$ and half duration $\Delta t = \sqrt{2\alpha}/\bar{\omega}$ verify $\Delta t \Delta\omega = 2$. For the lowest values of α, Eq. (11) has no physically meaningful carrier and envelope. With increasing α, Eq. (11) approaches a Gaussian-enveloped pulse of an increasing number of oscillations and Gaussian duration Δt, Φ becoming the carrier-envelope phase; e.g., a Gaussian-like, single-cycle pulse corresponds to $\alpha \simeq 13.75$. With this class of pulses, inequality (9) simply reads $|l| < 2\alpha$. For the pulse with $\alpha = 2.5$ in Ref. [19], we obtain $|l| < 5$, which is in line with the value $|l| < 4$ obtained in Ref. [19] for X waves, in spite of the different beam geometry. For the standard single-cycle pulse with $\alpha = 13.75$, $|l| < 27.5$; i.e., it can carry up to 27 units of OAM. The energy density of the RPB, normalized to its peak value at $z = 0$,

$$\mathcal{E}(r,z) = |D|^2 \left(\frac{2}{|l|}\frac{r^2}{s_{\bar{\omega}}^2(z)}\right)^{|l|} \left(\frac{\alpha}{\frac{r^2}{s_{\bar{\omega}}^2(z)} - \frac{|l|}{2} + \alpha}\right)^{2\alpha}, \tag{12}$$

is seen to feature for all $|l| < 2\alpha$ one and only one maximum at $r/s_{\bar{\omega}}(z) = \sqrt{|l|/2}$. For comparison with Figs. 2(a) and 2(b), the PE pulse in Fig. 2(c) is chosen to have $\alpha = 11.25$ so that inequality (9) yields the same limitation $|l| < 22.5$. The curves and vertical lines in Fig. 2(d) are the energy profiles with a single maximum at $r/s_{\bar{\omega}}(z) = \sqrt{|l|/2}$ up to $|l| = 22$ (instead of 18 in the preceding example) and with a minimum for $|l| > 22$ surrounded by infinite maxima, thus lacking physical meaning. Equation (9) being a sharp inequality for a class of pulses, it cannot be improved for general RPBs.

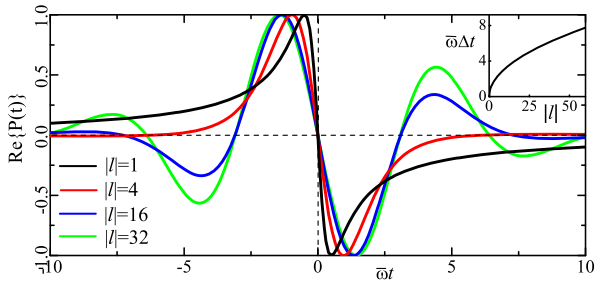

FIG. 3. Shortest l-vortex-carrying pulses. The higher the charge, the longer the minimum pulse duration $\Delta t = \sqrt{|l|}/\bar{\omega}$ needed, as seen in the inset.

For our last considerations, we note that the RPB (10) with the PE pulse (11) in its bright ring if $|l| < 2\alpha$ has the peculiarity of having the same PE pulse shape, i.e., the same α, at all caustics, being simply scaled to the blue-shifted [for $r/s_{\bar{\omega}}(z) < \sqrt{l/2}$] or redshifted [for $r/s_{\bar{\omega}}(z) > \sqrt{l/2}$] mean frequency $\bar{\omega}(r) = \bar{\omega}/\{1 - [r^2/s_{\bar{\omega}}^2(z) - |l|/2]/\alpha\}$. It then makes sense to talk about the pulse shape of the RPB as a whole.

An implication of the above results is that there exist minimal wave packets that can carry an l vortex and, in particular, a minimal wave packet that can carry a single vortex. Given $|l|$, the Gaussian-equivalent bandwidth of the pulse at the bright ring satisfies $\Delta\omega/\bar{\omega} < (2/\sqrt{|l|})$, an inequality saturated by the RPB with the PE pulse with $\alpha = |l|/2 + \epsilon$, $\epsilon \to 0$, of duration $\Delta t = 2/\Delta\omega$. We then obtain the inequality $\bar{\omega}\Delta t > \sqrt{|l|}$ limiting the duration of any RPB. Figure 3 shows shortest l-vortex-carrying pulses, that is, Eq. (11) with $\alpha = |l|/2 + \epsilon$, and their duration in the inset. At all caustics, the pulse shape is the same with the replacement $\bar{\omega} \to \bar{\omega}(r)$. These shortest, l-dependent RPBs can be also obtained by setting, as in Ref. [19], l-independent weights $\hat{a}_\omega \propto (\omega/\bar{\omega})^{\epsilon-1/2} e^{-\epsilon(\omega/\bar{\omega})}$ of the LG beam constituents. Coupling of the temporal and OAM degrees of freedom [19] makes the spectrum $\hat{P}_\omega \propto (\omega/\bar{\omega})^{\epsilon+|l|/2-1/2} e^{-(\epsilon+|l|/2)(\omega/\bar{\omega})}$, and the corresponding pulse shapes in Fig. 3, adapt to support the vortex of charge l.

In conclusion, settling a limit to the degrees of freedom of OAM in ultrashort pulses, or to the duration of pulses with OAM, has an impact in all fields where they are employed. In superdense optical communication systems, it implies a restriction to the OAM-based channels, and hence to their communication capacity [7], in quantum information, a limitation to multidimensional entanglement of OAM states for quantum cryptography [8]. Extreme ultraviolet attosecond pulses with high OAM generated via strong-field light-matter interactions [16,17] are also subject to these limitations, as well as, to mention a few waves of a different nature, electron beams with high OAM for electron microscopy [27] and ultrasound transient vortices in acoustics [28].

The author acknowledges support from Projects of the Spanish Ministerio de Economía y Competitividad No. MTM2015-63914-P and No. FIS2017-87360-P.

*miguelangel.porras@upm.es

[1] L. Allen, M. W. Beijersbergen, R. J. C. Spreeuw, and J. P. Woerdman, Phys. Rev. A **45**, 8185 (1992).
[2] A. M. Yao and M. J. Padgett, Adv. Opt. Photonics **3**, 161 (2011).
[3] G. Foo, D. M. Palacios, and G. A. Swartzlander, Opt. Lett. **30**, 3308 (2005).
[4] G. D. M. Jeffries, J. Scott Edgar, Y. Zhao, J. P. Shelby, C. Fong, and D. T. Chiu, Nano Lett. **7**, 415 (2007).
[5] H. He, M. E. J. Friese, N. R. Heckenberg, and H. Rubinsztein-Dunlop, Phys. Rev. Lett. **75**, 826 (1995).
[6] T. Omatsu, K. Chujo, K. Miyamoto, M. Okida, K. Nakamura, N. Aoki, and R. Morita, Opt. Express **18**, 17967 (2010).
[7] H. Huang *et al.* Opt. Lett. **39**, 197 (2014).
[8] G. Molina-Terriza, J. P. Torres, and L. Torner, Phys. Rev. Lett. **88**, 013601 (2001).
[9] A. B. Matsko, A. A. Savchenkov, D. Strekalov, and L. Maleki, Phys. Rev. Lett. **95**, 143904 (2005).
[10] K. Bezuhanov, A. Dreischuh, G. G. Paulus, M. G. Schtzel, and H. Walther, Opt. Lett. **29**, 1942 (2004).
[11] I. Zeylikovich, H. I. Sztul, V. Kartazaev, T. Le, and R. R. Alfano, Opt. Lett. **32**, 2025 (2007).
[12] Y. Tokizane, K. Oka, and R. Morita, Opt. Express **17**, 14517 (2009).
[13] V. G. Shvedov, C. Hnatovsky, W. Krolikowski, and A. V. Rode, Opt. Lett. **35**, 2660 (2010).
[14] K. Yamane, Y. Toda, and R. Morita, Opt. Express **20**, 18986 (2012).
[15] C. Hernández-García, A. Picón, J. San Román, and L. Plaja, Phys. Rev. Lett. **111**, 083602 (2013).
[16] G. Gariepy, J. Leach, K. T. Kim, T. J. Hammond, E. Frumker, R. W. Boyd, and P. B. Corkum, Phys. Rev. Lett. **113**, 153901 (2014).
[17] L. Rego, J. S. Román, A. Picón, L. Plaja, and C. Hernández-García, Phys. Rev. Lett. **117**, 163202 (2016).
[18] T. Brabec and F. Krausz, Phys. Rev. Lett. **78**, 3282 (1997).
[19] M. Ornigotti, C. Conti, and A. Szameit, Phys. Rev. Lett. **115**, 100401 (2015).
[20] M. Born and E. Wolf, *Principles of Optics* (Pergamon, Oxford, 1975).
[21] M. A. Porras, Opt. Lett. **34**, 1546 (2009).
[22] M. A. Porras, B. Major, and Z. L. Horvath, J. Opt. Soc. Am. B **29**, 3271 (2012).
[23] M. A. Porras, Phys. Rev. E **58**, 1086 (1998).
[24] M. A. Porras, J. Opt. Soc. Am. B **16**, 1468 (1999).
[25] S. Feng and H. G. Winful, Phys. Rev. E **63**, 046602 (2001).
[26] M. A. Porras, Phys. Rev. E **65**, 026606 (2002).
[27] B. J. McMorran, A. Agrawal1, I. M. Anderson, A. A. Herzing, H. J. Lezec, J. J. McClelland, and J. Unguris, Science **331**, 192 (2011).
[28] A. Marzo, M. Caleap, and B. W. Drinkwater, Phys. Rev. Lett. **120**, 044301 (2018).